

Chapter-6

Biogenic AuNPI3Cs produces oxidative stress and antiproliferation against Dalton's Ascitic Lymphoma (DLA) cells

6.1 Introduction

6.2 Materials and methods

6.3 Results

6.4 Discussion

6.5 Conclusion

Abstract

The present study was aimed to evaluate the anticancer activity of biogenic gold nanoparticles using indole-3-carbinol (AuNPI3Cs) against Dalton's ascites lymphoma (DLA) cells in *in vitro* and *in vivo* experimental conditions. Studies on cell viability, chromatin condensation using DAPI and PI staining and DNA fragmentation revealed that AuNPI3Cs were capable to produce significant anticancer and apoptotic effects on DLA cells. Studies on cellular redox balance, nitric oxide release level, reactive oxygen species formation and alteration of mitochondrial membrane potential confirmed the oxidative injury in DLA cells AuNPI3Cs. In cell cycle study, AuNPI3Cs induced apoptosis in DLA cells and there was significant cell cycle arrest at the G₀ /G₁ phase. To show the abilities in cancer chemoprevention, *in vivo* studies were also done in DLA-bearing Swiss albino mice. Significant reduction in body weight, tumour volume and tumour cell count and increase in mean survival time were observed. Remarkably AuNPI3Cs had no toxic effects on normal lymphocytes at doses up to 50 µg ml⁻¹. The results of this investigation clearly demonstrate that AuNPI3Cs inhibit the cell proliferation and survival of DLA cells via oxidative stress and induction of apoptosis in a dose-dependent manner.

6.1 Introduction:

Cancer is one of the most severe diseases that impair human health in the modern world and the second largest deadly disease after heart disease (Ma and Yu, 2006). Currently available anticancer drugs like alkylating agents, anti-metabolites, apoptosis inducers, cell cycle inhibitors and hormonal regulators are harmful to the normal cells. So, there is an amended interest in new drug of green origin as they are less to cause serious side effects (Babu et al., 1995).

6.1.1 Lymphoma and its treatments

According to the new World Health Organisation IV lymphoma classification system (Swerdlow et al., 2016), lymphomas are considered as a large and heterogeneous group of malignant diseases of lymphoid tissue which consists of 70 different subtypes. Hodgkins lymphoma (HL) and non-Hodgkin lymphoma (NHL) are two major categories of lymphoma (Seam et al.,2007).

T cell lymphomas are a type of malignancy of the immune system that affects 15,884 males and 7,918 females per 100,000 in India. The rate of NHL mortality for male and female were 11,071 and 5,526 per 100,000 respectively (State of Healthcare in India - Lymphoma Coalition, 2015). B- and T-cell lymphomas are the more common Non-Hodgkin lymphomas which depends on the cell type of origin. At various stages of differentiation T-cell lymphomas are clonal tumours of immature or mature T lymphocytes. They account for only 10-12% of all NHLs, the rest being of B-cell origin.

The clinical appearance of lymphomas is often a swollen lymph node in the neck, axilla, but several other are common. Standard treatment for lymphomas is combination chemotherapy for repeated times. For B-cell lymphomas, the addition of an anti-CD20 antibody has produced improved outcome noticeably and is now a part of the standard treatment. By this

treatment lesser outcome is seen in T-cell lymphomas than lymphomas of B-cell origin (Gisselbrecht et al., 1998) and continuous effort is put into finding new treatment modalities or efficient combinations of existing treatments. Addition of an anti-CD52 antibody and high-dose chemotherapy with stem cell rescue are currently being tested in clinical trials for T-cell lymphomas. Radiation therapy is also important in lymphoma treatment, both with curative and comforting intention (Li et al., 2006). T-cell lymphomas resemble stages of normal T-cell differentiation and some of them can be classified according to the corresponding normal stage. The cells of the adaptive immune system are T and B lymphocytes, allow highly specific and strong response to pathogen. From different research studies it is revealed that the mice affected by the disease showed enlargement of lymph nodes, spleen, liver, thymus and kidneys. Histopathologic analysis showed the morphological appearance of medium sized monotonous lymphoblast (Coustan-Smith et al., 2009).

6.1.2 Dalton ascites lymphoma (DLA) cell

Dalton's lymphoma is an established transplantable tumour model which is well characterized and reproducible and traditionally have been used for the study of local tumour growth and predictable survival period (Sriram et al., 2010) as well as the model cell line for drug development. Dalton's lymphoma (DL) ascites tumorigenesis model in mice provides a convenient model system to study such effects *in vivo* system (Shanker et al., 2000).

6.1.3 Dalton's ascites lymphoma model to study the antiproliferative role of medicinal plants

Methanol extract of *Cissam pelospariera* (MECP) was reported to show a potent cytotoxic activity against DLA cells and caused a significant decrease in packed cell volume, viable cell count, and an increase in lifespan in DLA-bearing mice. The altered haematological and

serum biochemical profiles and antioxidant enzymes were restored to normal levels in MECP-treated mice (Samuel et al., 2014). Ethanolic and aqueous extracts of *Vitex negundo* Linn. leaf exhibited antitumor efficacy against DLA cells (Dewade et al., 2010). Ethanolic extract of *Dendrobium formosum* caused apoptosis and arrested the DLA cell cycle at G₂/M phase (Prasad and Koch, 2014). Different doses of ethanolic extract of *Cnidioscolus chayamansa* was reported to decrease the body weight, reduced the packed cell volume (PCV), viable tumor cell count and increased the life span of DLA treated mice and brought back the haematological parameters, serum enzyme and lipid profile near to normal values (Kulathuranpillai et al., 2012).

Although, plant extract/phytochemicals are of great importance for the cancer treatment but there are some limitations due to their poor bioavailability and solubility (Aqil et al., 2013). In this scenario, nanotechnology play a vital and noteworthy role to overcome the limitations of conventional treatment. Plant extracts have excellent properties for the synthesis of novel nanoparticles, including gold (Thakkar et al., 2010). Biosynthesis of nanoparticles by plant extract/ phytochemicals has several advantages and cost effectiveness with high efficacy (Singhal et al., 2011).

Till now very little is known regarding the anticancer activity of biosynthesized gold nanoparticles as well as its specific mechanism of action on T-cell lymphomas.

In this section, the present study was designed to explore the mechanistic basis of apoptosis producing, anti-proliferative and antioxidant activity of green-synthesized gold nanoparticles (AuNPI3Cs) against DLA cell *in-vitro* and *in-vivo* condition.

6.2 Materials and methods

6.2.1 Chemicals and reagents

Sodium dodecyl sulphate (SDS), Ethylene diamine tetraacetic acid (EDTA), Tris buffer, sodium azide, thioburbituric acid (TBA), tricarboxylic acid (TCA), dimethyl sulfoxide (DMSO), Tris-HCl, citric acid, trypsin, calcium chloride (CaCl₂), hydrogen peroxide (H₂O₂), hydrochloric acid (HCl), reduced glutathione (GSH), sulfosalicylic acid, pyrogallol, sodium hydrogen phosphate (Na₂HPO₄), 1-Chloro-2, 4 dinitrobenzene (CDNB), 5-fluorouracil and other chemicals were purchased from Sigma-Aldrich, St. Louis, MO, USA and Merck India, Ltd., Mumbai, India.

6.2.2 Animal maintenance

Animal maintenance was described in chapter 5. DLA cell lines were maintained weekly through intraperitoneal inoculation at the concentration of 1×10^6 /cells per mouse.

The study was permitted by the Institutional Animal Ethical Committee, registered under CPCSEA (approval No. IEC/7-14/C14-16).

6.2.3 Cancer cell culture

Dalton ascites lymphoma (DLA) cells were also obtained from Chittaranjan National Cancer Institute, Kolkata. Cells were grown in DMEM medium comprising 10% FBS and antibiotics in appropriate conditions and were maintained by intraperitoneal inoculation (2×10^6 /cells/mouse) in the above said mice. After PBS washing, cells were cultured in DMEM medium added with 10% foetal bovine serum (FBS) and antibiotic solution (100 U

ml⁻¹ penicillin, 10 mg ml⁻¹ streptomycin and 4 mM L-glutamine) under 5% CO₂ and 95% humidified atmosphere at 37⁰C in a CO₂ incubator and used for different experiments.

6.2.4 Isolation of mouse lymphocytes

Mice lymphocytes were isolated as described in chapter-3.

6.2.5 Experimental Design

In vitro cytotoxicity of AuNPI3Cs was performed against DLA cells. DLA (1× 10⁶ cells ml⁻¹) cells were treated with AuNPI3Cs at different concentrations (0.5, 1, 2, 5, 10, 25µg/ml) for 24 h. After the treatment, the cells were collected from the culture plates. DLA cells were washed two times by 0.1 M PBS (pH 7.4) at 1200 rpm for 5 min at 4°C. Then washed DLA cells were used for the measurement of different oxidative stress and apoptosis biomarkers.

6.2.6 *In vitro* cytotoxicity study by MTT assay

The method has been described previously in chapter 4. The effect of AuNPI3Cs on the proliferation of DLA cells were expressed as the % of cell viability using the following formula:

$$\% \text{ cell viability} = [\text{OD sample} - \text{OD control}] \times 100 / \text{OD control}$$

6.2.7 Estimation of reduced glutathione (GSH)

The procedure as same as described earlier in chapter 4 (Griffith 1981).

6.2.8 Determination of oxidized glutathione (GSSG)

The oxidized glutathione level was performed according to the modified method of Griffith, 1980 has been previously described in chapter 4.

6.2.9 Intracellular ROS measurement

Intracellular ROS measurement (Roy et al.,2008) was previously described in chapter 4.

6.2.10 Chromatin condensation by PI and DAPI staining

The method has been previously described in chapter 4.

6.2.11 Acridine orange–ethidium bromide double staining

The method has been previously described in chapter 5.

6.2.12 DNA fragmentation study by agarose gel electrophoresis

The procedure has been described in chapter 3 (Gong et al.,1994).

6.2.13 Measurement of Mitochondrial membrane potential ($\Delta\Psi_m$)

The method has previously described in chapter 4 (M'memba et al., 2006).

6.2.14 Analysis of cell cycle disruption by flow cytometry

The method of cell cycle analysis by flow cytometry (Evans et al.,2000) has been described in chapter 4.

6.2.15 *In vivo* study

Forty eight male mice were divided into four groups containing twelve in each group except Group I having six mice.

Group IA : Saline control

Group IIA : DLA control

Group IIIA : DLA + I3C (75mg/kg body weight)

Group IVA : DLA + I3C (150mg/kg body weight)

Group IIIB : DLA + AuNPI3Cs (2mg/kg body weight)

Group IVB : DLA + AuNPI3Cs (4mg/kg body weight)

Group V : DLA + 5-FU (20 mg/kg body weight)

Animals of all groups were taken 0.1 ml of 1×10^6 DLA cells/mouse intraperitoneally except Group I and this was taken as day zero. Group IIA and group IIB were served as tumor

control groups. Groups III and IV were injected intraperitoneally with I3C and AuNPI3Cs in two doses respectively and group V received reference drug 5-FU respectively once daily for 14 consecutive days after 24 h of tumour inoculation (Halder et al., 2010). The body weight changes of the animal were recorded daily from the day of zero to the last day (Maiti et al., 2010). Blood was collected via cardiac puncture from six mice of each group for the estimation of haematological parameters. For the study of tumour regression parameters ascites fluid was drawn from peritoneal cavity (Gupta et al., 2004). For the study of hepatic and renal oxidative stress parameters study, liver and kidney tissue was collected. To record the mean survival time, the remaining alive 6 mice of Group III - V each were checked on a daily basis.

6.2.16 Changes in Body weight

Thirty male mice were taken to observe body weight change and divided into five groups (n=6). Tumour growth was observed in terms of daily body weight change and recorded from the day of zero to the last day (Maiti et al., 2010).

6.2.17 Studies on host survival time and increase life span

The method has been described in chapter-5.

6.2.18 Tumour volume

The method has been previously discussed in chapter-5.

6.2.19 Tumour cell count

The method has been described in chapter-5.

6.2.20 Heamtological analysis

RBC, WBC count was done by the methods of Wintrobe, 1967 and haemoglobin percentage has been determined by cyanmethaemoglobin method (Dacie and Lewis, 1975) as described in chapter 3.

6.2.21 Antioxidant Parameters

Estimation of malondialdehyde (MDA) content, reduced glutathione (GSH), superoxide dismutase (SOD), catalase (CAT) have been described in chapter 5.

6.2.22 Statistical analysis

All the experiments were done in triplicate manner. The results were expressed as Mean \pm SEM. Comparisons between the means of the control and treated groups were calculated by using the one-way ANOVA test (using a statistical package, Origin 6.1, Northampton, MA), $p < 0.05$ as a limit of significance.

6.3. Results

6.3.1 Effect of AuNPs and AuNPI3Cs on *in vitro* cytotoxicity against DLA cells.

The dose-dependent *in vitro* cytotoxicity was noticed (Figure 6.1) in AuNPI3Cs treated DLA cells. DLA cell viability was decreased significantly 3%, 9.69%, 15.86%, 49.75%, 58% and 68.78% by AuNPI3Cs at 0.5, 1, 2.5, 5, 10 and 25 $\mu\text{g ml}^{-1}$. The viability of MLC was also not significantly altered up to 25 $\mu\text{g ml}^{-1}$ dose level of AuNPI3Cs (Figure 6.1). At IC_{50} values (10 $\mu\text{g ml}^{-1}$) of AuNPI3Cs for DLA cells, no *in vitro* cytotoxicity was shown in mouse lymphocytes. So, our further experiments on DLA cells were carried out using these respective IC_{50} concentrations. But after treatment of chemically synthesized AuNPs, cell viability of mice lymphocytes were reduced significantly as well as cancer cells.

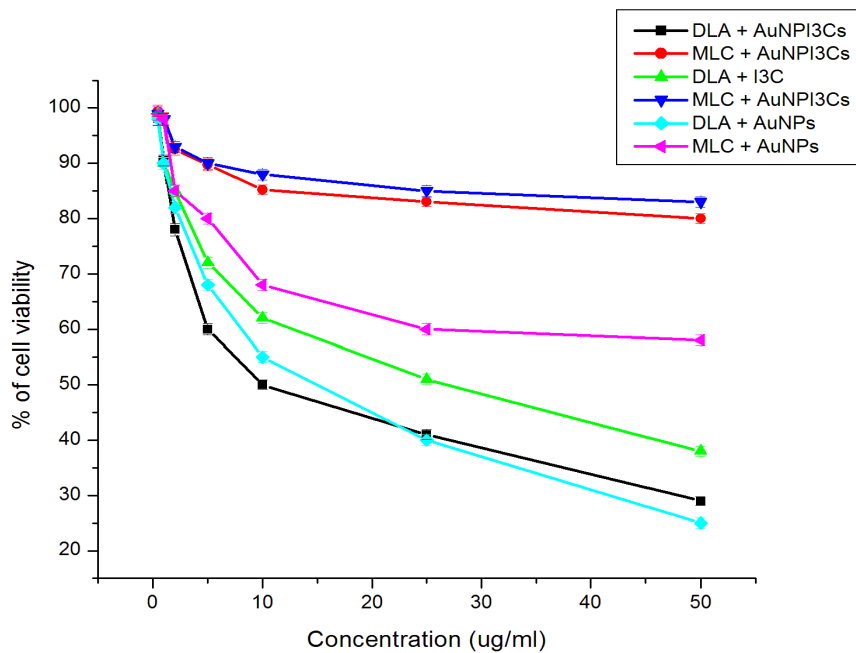


Figure 6.1. Effect of AuNPI3Cs on *in vitro* cytotoxicity against DLA cells and MLCs. Cells were treated with AuNPI3Cs for 24 h at 37°C. Values are expressed as Mean±SEM of three experiments.

6.3.2 Effect of AuNPI3Cs on GSH and GSSG content of DLA cells

The present study revealed that the levels of GSH in DLA cells by 5-FU and AuNPI3Cs (Figure 6.2). AuNPI3Cs significantly ($p < 0.001$) diminished the GSH level of DLA cells at IC_{50} dose. The level of GSSG was increased in AuNPI3Cs and 5-FU treated DLA cells at IC_{50} dose (Figure 6.2).

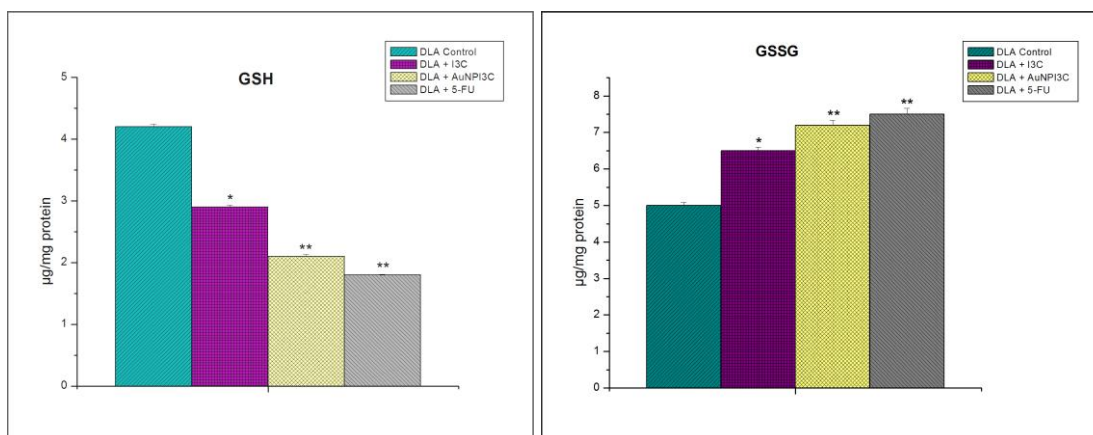


Figure 6.2a: Intracellular reduced glutathione (GSH) levels of DLA cells. 6.2b: Intracellular oxidized glutathione (GSSG) levels of DLA cells. The levels of GSH were expressed as μg of GSH mg^{-1} protein. The levels of GSSG were expressed as μg of GSSG mg^{-1} protein. Cells were treated with AuNPI3Cs and 5-FU for 24 h at 37°C . Values are expressed as Mean \pm SEM of three experiments. ; ‘*’ indicates a statistically significant difference ($p<0.05$) ‘**’ indicates a statistically significant difference ($p<0.01$), compared with DLA control group.

6.3.3 Effect of AuNPI3Cs on ROS generation in DLA cells

In DLA cells, DCF fluorescence intensity caused by ROS generation was elevated after AuNPI3Cs treatment. AuNPI3Cs caused increased ROS production as shown by increased DCF staining in the nucleus (Figure 6.3).

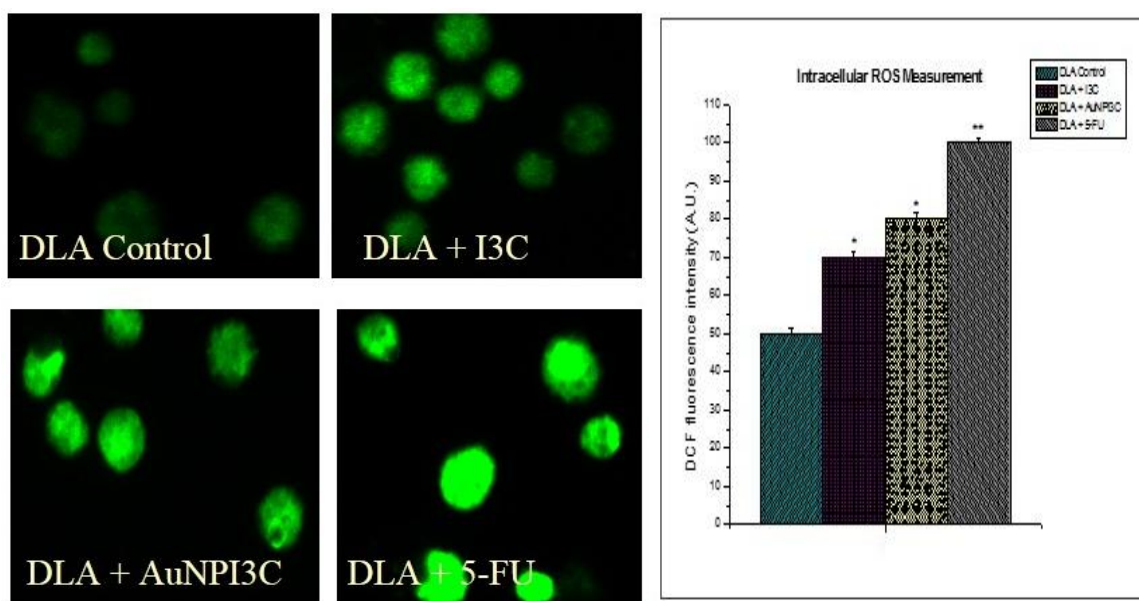


Figure 6.3a: Effects of AuNPI3Cs and 5-FU on reactive oxygen species (ROS) induction in DLA cell line; Qualitative characterization of ROS formation by H_2DCFDA staining using fluorescence microscopy. (a) DLA control (b) I3C treated (c) AuNPI3Cs treated (d) 5-FU treated. 6.3b: DCF fluorescence intensity of DLA cells were expressed in graphical form in term of ROS production. Values are expressed as Mean \pm SEM of three experiments; ‘**’

indicates a statistically significant difference ($p < 0.001$); ‘***’ indicates a statistically significant difference ($p < 0.001$), compared with control.

6.3.4 Effect of AuNPI3Cs on chromatin condensation in DLA cells

In the control group, cells displayed a round shape, and large nuclei were homogenously stained with a less bright red and blue color. After PI staining, red light emitted from the AuNPI3Cs treated DLA (Figure 6.4A) cells. Cells were much brighter and condensed compared to the control. However, the blue emission from the treated cells after DAPI staining was much brighter and condensed compared to DLA control (Figure 6.4B) cells.

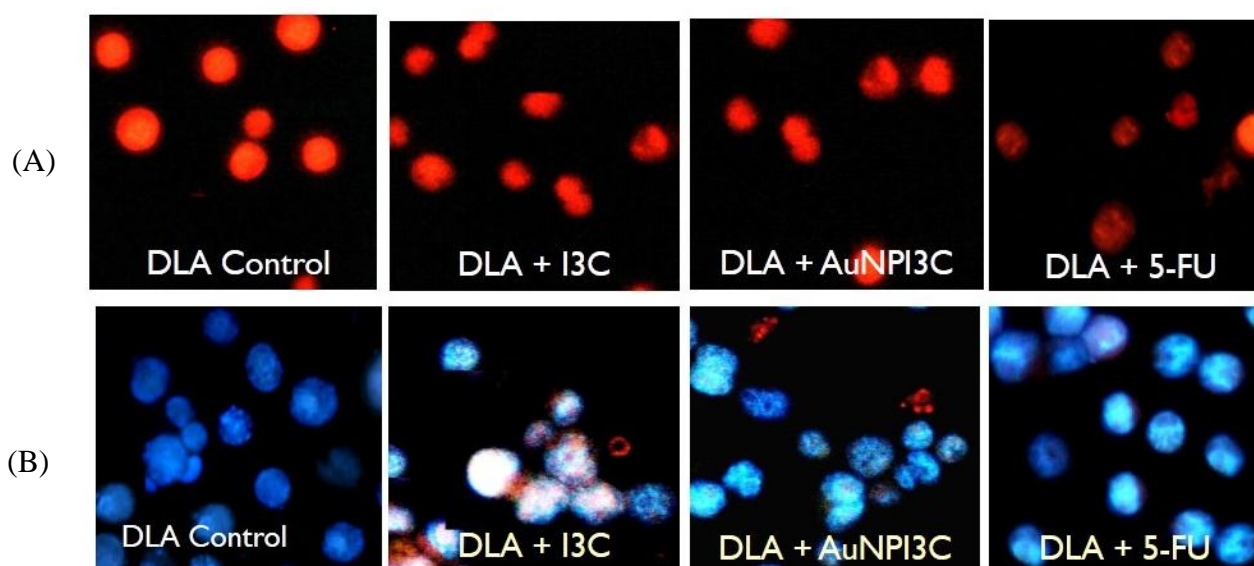


Figure 6.4. Fluorescence- based chromatin condensation study. A. Cells were stained with propidium iodide (PI) B. Cells were stained with DAPI and visualized under a fluorescence microscope to detect chromatin condensation. Here, (a) Control DLA cells, (b) I3C treated DLA cells (c) AuNPI3Cs treated DLA cells (d) 5-FU treated DLA cells.

6.3.5 AO-EtBr staining in DLA cells

As shown in Figure 6.5, all the morphological changes were observed in treated DLA cells. In the control group, green live DLA cells with normal morphology were detected and

AuNPI3Cs treated early apoptotic DLA cells with yellow green nuclei as well as late apoptotic cells with orange nuclei were seen in 5-FU treated group.

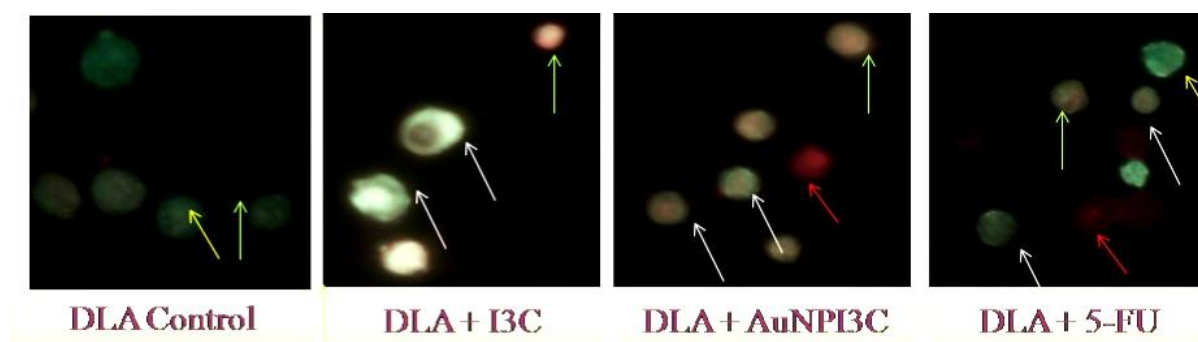


Figure 6.5. Figure 6.5. EtBr-AO double staining of DLA cells under fluorescence microscope.

Here, (a) Control DLA cells, (b) I3C treated DLA cells (c) AuNPI3Cs treated DLA cells (d) 5-FU treated DLA cells. White arrow indicates viable cell, yellow arrow indicates early apoptotic cell, blue arrow indicates late apoptotic cell and red arrow indicates necrotic cell.

6.3.6 DNA fragmentation study by gel eletrophoresis

From the gel electrophoresis it was revealed that DNA of AuNPI3Cs treated DLA (Figure 6.6) cells displayed smear like pattern compared to control.

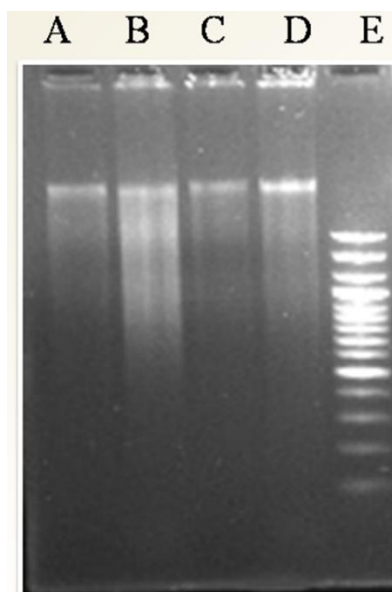


Figure 6.6. Shows the effect of AuNPI3Cs, I3C and 5-FU on DNA fragmentation. Here, (A) 5-FU-treated DLA cell; (B) AuNPI3Cs-treated DLA cells; (C) I3C-treated DLA cells; (D) DLA control and (E) 100 bp DNA ladder.

6.3.7 Effect of AuNPI3Cs in Mitochondrial membrane potential ($\Delta\Psi_m$)

In this study, it was found that at IC_{50} dose AuNPI3Cs caused significant depletion of MMP ($p < 0.001$) in DLA cells compared to control. The mitochondrial membrane potential was estimated based on rhodamine 123 fluorescence intensity. The percentage of MMP decreased significantly ($p < 0.001$) in DLA cells when treated with IC_{50} dose of AuNPI3Cs.

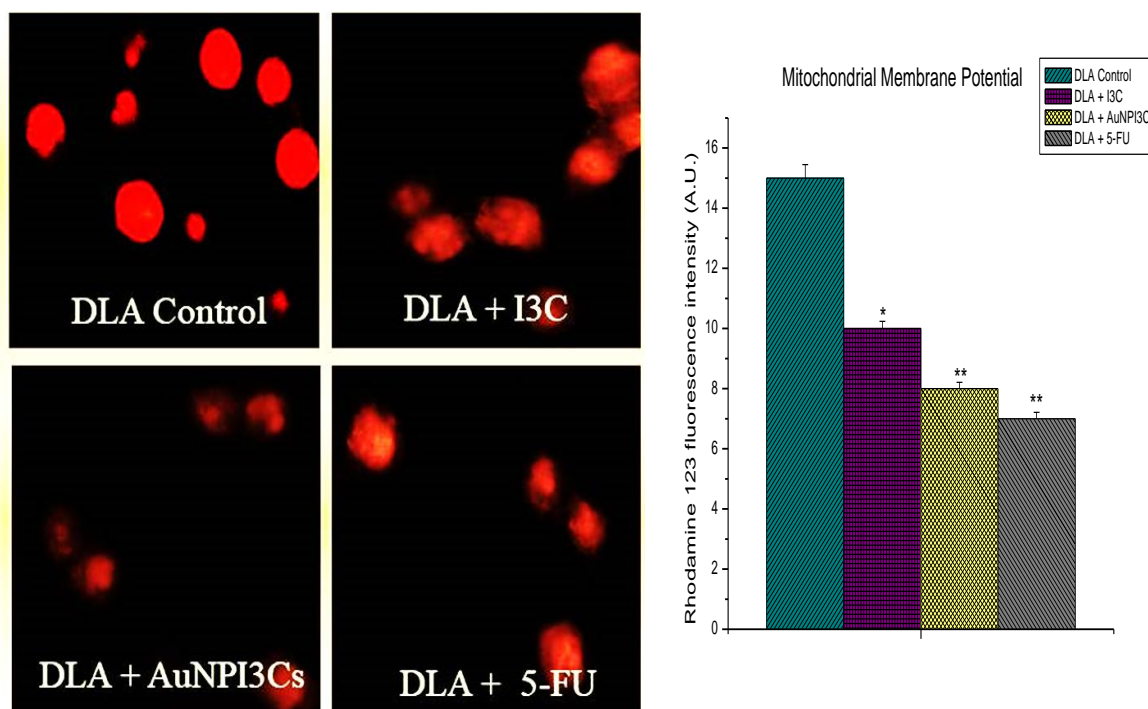


Figure 6.7. A. Measurement of mitochondrial membrane potential (MMP) of AuNPI3Cs and 5-FU treated DLA cells. Values are expressed as Mean \pm SEM of three experiments; ‘*’ indicates a statistically significant difference ($p < 0.05$), compared with control. ‘**’ indicates a statistically significant difference ($p < 0.01$), compared with control. (a) DLA control (b) I3C-treated DLA cells, (c) AuNPI3Cs-treated DLA cells, (d) 5-FU treated DLA cells. B. Qualitative characterization of mitochondrial membrane potential by Rhodamine 123 staining using fluorescence microscopy.

6.3.8 Flow cytometry–based analysis of cellular apoptosis

Cells were treated with the IC_{50} concentrations of AuNPI3Cs for 24 h. DNA content of treated DLA cells were examined by using PI staining and cell distributions among sub-G1, G0/1, S and G2/M phases were analysed. (Figure 6.8). The present result showed that G0/G1 phase DLA cells was significantly higher in AuNPI3Cs treated group than DLA control group.

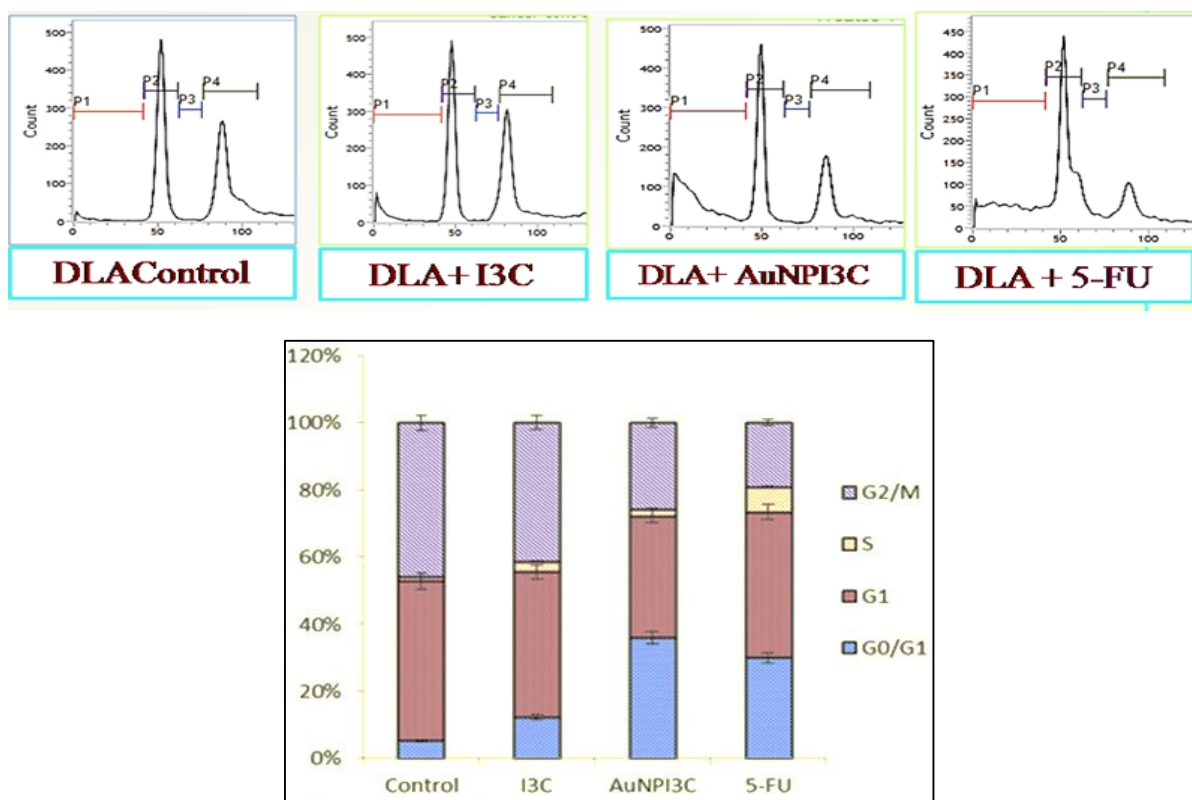


Figure 6.8. Cell cycle arrest analysis by flow cytometry. Cells were treated with AuNPI3Cs and 5-FU for 24 h, stained with PI and measured by flow cytometry (A) Fluorescence activated cell sorting study was done to observe the cell distributions among sub-G₀, G₀/G₁, S and G₂/M phases in DLA cells. (a) DLA control (b) I3C-treated DLA cells, (c) AuNPI3Cs-treated DLA cells, (d) 5-FU treated DLA cells. (B) Graph shows the percentage of DLA cells in different phases of cell cycle from flow cytometric analysis.

6.3.9 Effect of AuNPI3Cs on tumor growth of DLA-bearing mice

6.3.9.1 Effect of AuNPI3Cs in body weight change of tumour bearing mice

Body weight of the mice increases significantly in DLA control group compared to control group, but in I3C and AuNPI3Cs treated groups at doses 2/4 mg/kg bwt the body weight was decreased significantly compared to DLA control group (Figure 6.9).

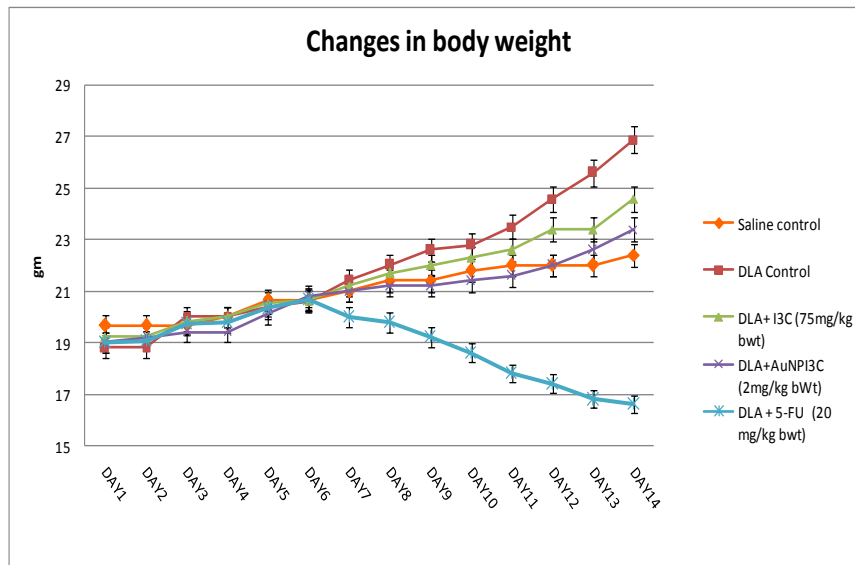


Figure 6.9. The effect of AuNPI3Cs on change of body weight of DLA bearing mice. Data are expressed as Mean± SEM.

6.3.9.2 Effect of AuNPI3Cs in survival loss, increase life span and mean survival time of tumour bearing mice

Treatment with I3C and AuNPI3Cs at the doses of 75 mg/kg bwt and 2 mg/kg bwt respectively increased the mean survival time (MST) (Figure 6.10) by 20 ± 1.1 , 32 ± 1.05 days, respectively compared to DLA control group.

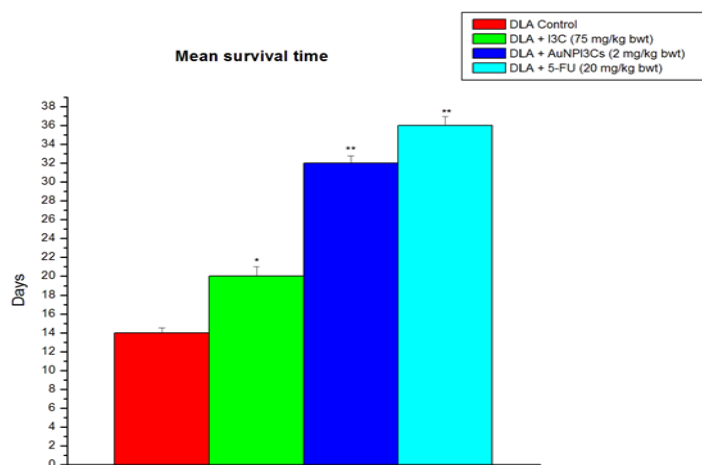


Figure 6.10. The effect of AuNPI3Cs on Mean survival time in DLA bearing mice. Data are expressed as Mean \pm SEM.

6.3.9.3 Effect of AuNPI3Cs in tumour volume and tumour cell count in DLA bearing mice

AuNPI3Cs treatment significantly reduced tumour volume (Figure 6.11) and tumour cell count (Figure 6.12) compared to DLA control mice.

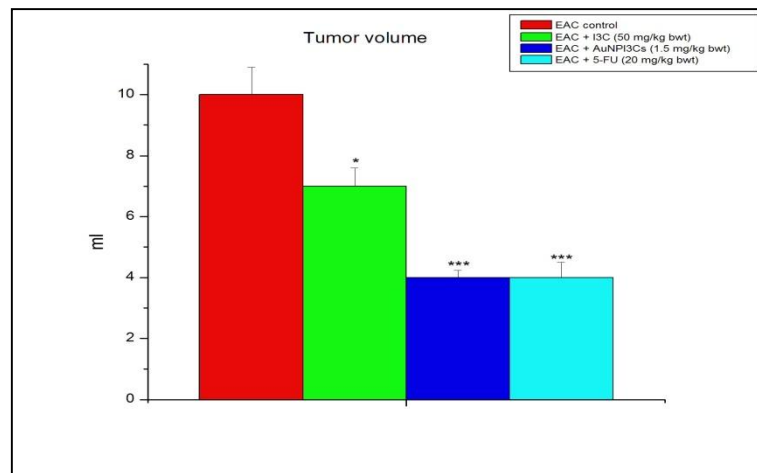


Figure 6.11. The effect of AuNPI3Cs on tumour volume in DLA bearing mice. Data are expressed as Mean \pm SEM. Probability values are given in asterisks. ‘*’ indicates significantly difference $p < 0.05$; ‘***’ indicates $p < 0.001$; probability values are determined in respect of DLA control.

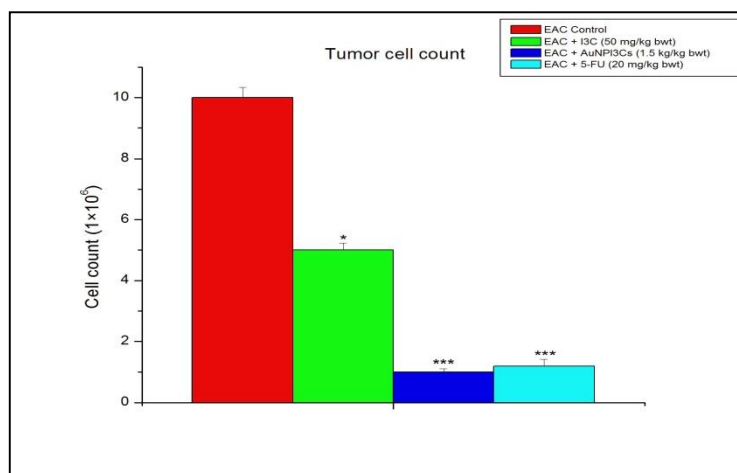


Figure 6.12. The effect of AuNPI3Cs on tumour cell count in DLA bearing mice. Data are expressed as Mean \pm SEM. ‘*’ indicates significantly difference $p < 0.05$; ‘***’ indicates $p < 0.001$; probability values are determined in respect of DLA control.

6.3.10 Effect of AuNPI3Cs on hematological parameters

The hematological parameters were altered significantly ($p < 0.001$) after 14 days of treatment with I3C and AuNPI3Cs when compared to DLA (Table 6.1) control group. It was found that total WBC count was increased significantly in DLA control group whereas, the hemoglobin percentage and RBC count were decreased significantly in the tumour control group. After treatment of AuNPI3Cs for 14 days, at doses of 2 and 4 mg/kg in DLA bearing mice, hematological parameters were brought back towards normal level. These results suggested that AuNPI3Cs have protective role on haemopoietic system. However, the standard drug 5-FU (20 mg/kg body weight) exhibited significant ($p < 0.001$) results in all these haematological parameters.

Table 6.1 Effect of I3C and AuNPI3Cs on haematological parameters in DLA bearing mice

Hematological Parameters	Saline Control	DLA Control	DLA + I3C (75 mg/kg bwt)	DLA + I3C (150 mg/kg bwt)	DLA + AuNPI3Cs (2 mg/kg bwt)	DLA + AuNPI3Cs (4 mg/kg bwt)	DLA+ 5-FU (20 mg/kg bwt)
Hb percentage	12.65±0.17	7.7±0.15 a***	9.5±0.15 a*b*	10.56±0.13 a*b**	11.58±0.17 b***	12±0.15 b***	12.35±0.17 b***
Total RBC count (×10 ⁶ mm ³)	6.5±0.08	1.85±0.05 a***	4.8±0.06 a*b***	5.2±0.05 a*b***	5.8±0.02 b***	6.0±0.00 2 b***	6.1±0.017 a* b***
Total WBC count (/μl)	4100±32	8200±10 a***	6200±52 a**b**	6000±40 a**b***	5800±55 a**b***	5000±24 b***	4800±28 b***

Data are expressed as Mean± SEM (n=6). a***'represents significant difference at (p<0.001) compared to saline control; 'b**' represents significant difference at (p<0.01); 'b***''represents significant difference at (p<0.001) compared to DLA control.

6.3.11 Effect of AuNPI3Cs on antioxidant parameters

The level of lipid peroxidation in liver and kidney tissue was significantly increased in tumour control mice when compared to saline control mice. After administration of AuNPI3Cs (2 and 4 mg/kg bwt) in DLA bearing mice, lipid peroxidation levels were significantly decreased when compared with DLA control mice. Reduced glutathione level (GSH) were changed in tumour control compared to saline control, restored to the normal values after treatment with AuNPI3Cs as well as 5-FU. In tumour control mice there were significant reduction in antioxidant enzymes like super oxide dismutase (SOD), catalase which were significantly improved by the treatment of AuNPI3Cs as well as 5-FU. GPx and GST levels both were decreased significantly in tumour control group, AuNPI3Cs treatment increased significantly.

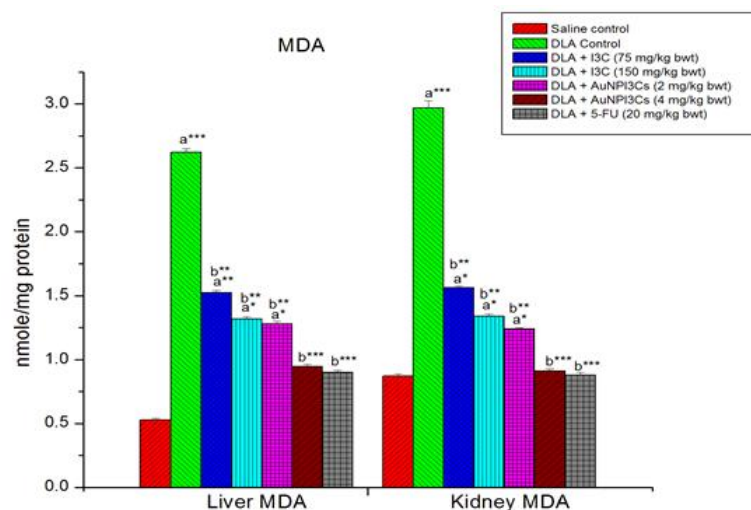


Figure 6.13 shows the effect of AuNPI3Cs on liver and kidney MDA after 15 days treatment in DLA bearing mice. Data are expressed as Mean \pm SEM (n=6). a***' represents significant difference at (p<0.001) compared to saline control; 'b**' represents significant difference at (p<0.01); 'b***' represents significant difference at (p<0.001) compared to DLA control.

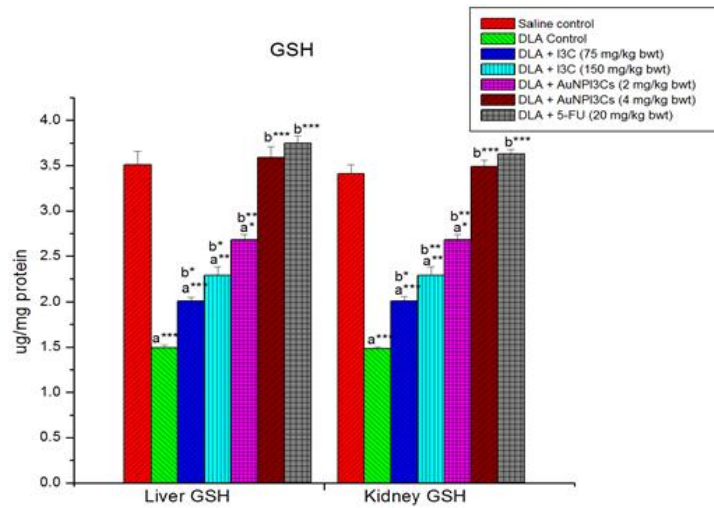


Figure 6.14 shows the effect of AuNPI3s on liver and kidney GSH after 15 days treatment in DLA bearing mice. Data are expressed as Mean± SEM (n=6). a***'represents significant difference at (p<0.001) compared to saline control; 'b**' represents significant difference at (p<0.01); 'b***' represents significant difference at (p<0.001) compared to DLA control.

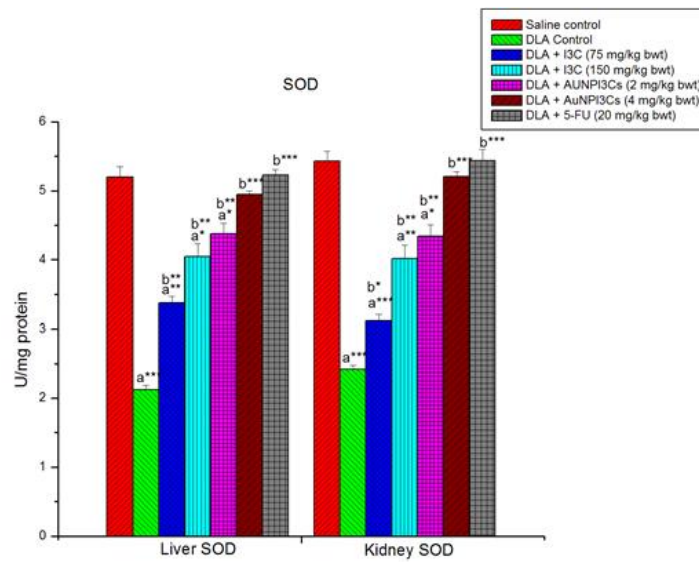


Figure 6.15 shows the effect of AuNPI3Cs on liver and kidney SOD after 15 days treatment in DLA bearing mice. Data are expressed as Mean± SEM (n=6). a***'represents significant

difference at ($p < 0.001$) compared to saline control; ‘b**’ represents significant difference at ($p < 0.01$); ‘b***’ represents significant difference at ($p < 0.001$) compared to DLA control.

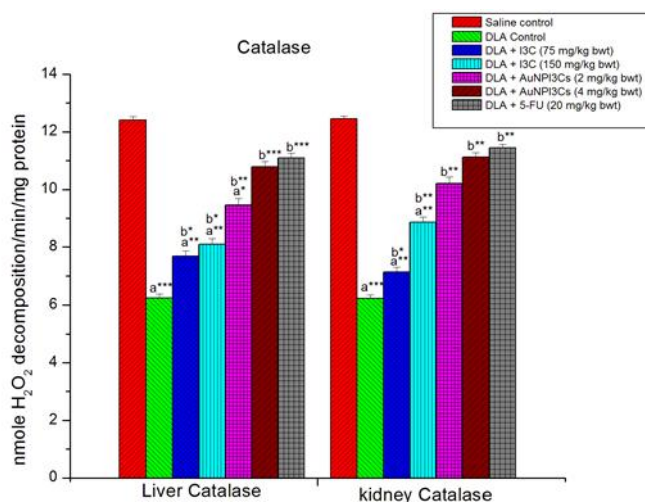


Figure 6.16 shows the effect of AuNPI3Cs on liver and kidney Catalase after 15 days treatment in DLA bearing mice. Data are expressed as Mean \pm SEM (n=6). a***’ represents significant difference at ($p < 0.001$) compared to saline control; ‘b**’ represents significant difference at ($p < 0.01$); ‘b***’ represents significant difference at ($p < 0.001$) compared to DLA control.

6.4. Discussion

The present study was aimed at analyzing the anticancer activity of gold nanoparticles using indole-3-carbinol (AuNPI3Cs) against DLA cells in *in-vitro* and *in-vivo* condition.

At IC₅₀ value (10 $\mu\text{g ml}^{-1}$) of AuNPI3Cs, no trace of cytotoxicity was observed in human lymphocytes. These data created interest as it suggested that AuNPI3Cs were more toxic to cancer cells compared to normal cells (Figure 6.1).

Cellular GSH level is decreased for the oxidation of reduced glutathione to glutathione disulphide (GSSG) in many pathological conditions. In oxidative stress, the conversion of GSH to GSSG is enhanced (Gr̃avil̃a et al., 2010).

The present study revealed the decreased GSH (Figure 6.2a) and increased GSSH (Figure 6.2b) levels in AuNPI3Cs treated DLA cells. So, by altering the intracellular redox status, AuNPI3Cs may decrease DLA cell viability.

Reactive oxygen species (ROS) generation has an imperative role in apoptosis mediated cancer cell death (MateÂs and SaÂnchez-JimeÂnez, 2000). ROS play a vital role in cell signalling, leading to oxidative stress due to unpaired valence shell electrons (Davies, 2000). Intracellular ROS generation occurs from mitochondrial respiratory chain reaction and membrane-bound superoxide-generating enzyme i.e., nicotinamide adenine dinucleotide phosphate (NADPH) oxidase mediated reactions. After exposure to AuNPI3Cs for 24 h, DLA cells showed (Figure 6.3) enhanced ROS formation as shown by the increased DCF fluorescence intensity.

Chromatin condensation is an important characteristic of apoptosis (Hacker,2000). After staining with PI and DAPI it had been exhibited that I3C and AuNPI3Cs induced several features of apoptosis such as condensed chromatin and fragmented punctuate red and blue nuclear fluorescence in EAC cells (Figure 6.4A and 6.4B). As membrane integrity became compromised; PI and DAPI stain dripped into intact membrane, even in shrunken cell, the apoptotic nuclei appeared bright pink and bright blue chromatin that are highly condensed and fragmented (Bortner and Cidlowski, 1998).

The cells which have intact DNA and nuclei have a round and green nucleus is recognized as viable cells. Early apoptotic cells possess appeared with yellowish green coloured nuclei. Late apoptotic and necrotic cells were stained orange and red respectively. From Figure 6.5,

it is clearly obvious that AuNPI3Cs caused cell death through apoptosis nor necrosis. Because most of the AuNPI3Cs treated cells showed features of late apoptotic and minimum number of cells necrosis (Suman et al.,2012).

ROS can act as signal molecules promoting cell-cycle progression and induce oxidative DNA damage. DNA fragmentation is generally considered a characteristic feature of apoptosis. Induction of apoptosis can be established by two reasons: in which the cells are reduced and condensed, and DNA fragmentation (Sohaebuddin et al., 2010). To confirm the apoptotic features induced by AuNPI3Cs, a DNA fragmentation assay was conducted. Figure 6.6 clearly indicates AuNPI3Cs induced cell death.

From the comet assay it was shown that AuNPI3Cs caused significant rise in tail DNA intensity percentage in DLA cells compared to DLA control. Direct induction of DNA strand breaks or disruption of DNA backbones by nanoparticles or it's by products can increase in the tail DNA percentage (Dash et al., 2014). AuNPI3Cs may readily cross the nuclear membrane and then directly or indirectly interact with DNA (Asare et al., 2012).

Decreased of MMP in DLA cell suggested a possible disruption of the cellular mitochondrial membrane after AuNPI3Cs treatment. Alteration of $\Delta\Psi_m$ in AuNPI3Cs-treated cells may result in malfunction in ATP synthesis and maintenance of ATP level that leads to apoptosis. Cellular apoptosis does not depend only on ATP synthesis depletion, whereas a lowered level of ATP triggers apoptosis induced cell death (Adrie et al., 2001).

Results revealed increasing accumulation of cells at the G0/G1 phase. Accumulation of G0/G1 phase cells was significantly greater in AuNPI3Cs treated DLA cells than DLA controls. Cells have mechanisms to continue genomic stability through cell cycle arrest (Xue et al.,2012). It is evident that alteration in cell cycle checkpoints cause cell cycle arrest which leads to apoptosis (Davis et al.,2009).

The body weight of AuNPI3Cs treated mice was decreased compared to control DLA bearing mice. Tumour volume and tumour cell count also decreased in AuNPI3Cs-treated tumour bearing mice. This reduction could be positively correlated with the ascites fluid volume or tumour volume. Ascites fluid provides the nutritional source for tumour cells (Prasad and Giri, 1994). Prolongation of life span is a reliable criterion to evaluate an anticancer drug (Rajesh et al., 2011). With reliability to this, average life span of AuNPI3Cs treated mice increased considerably.

Malondialdehyde (MDA) is an end product of oxidative degeneration has been reported to be higher in cancer tissues (Valenzuela, 1991). The levels of MDA were found to be rapidly increased in DLA induced mice and returned back near to normal after treatment of AuNPI3Cs. Glutathione provide intracellular protection against free radicals, peroxide and toxic compounds. Tumour progression markedly reduced cellular GSH, which may be due to oxidative stress (Grăvilă et al., 2010). Decreased levels of GSH might be as a result of the effective conversion of GSH to GSSG by increased free radicals in tumour cells. Significant improvement in liver and kidney GSH was achieved by the treatment of AuNPI3Cs and I3C, signifying the protective role of AuNPI3Cs and I3C in DLA bearing mice. The levels of antioxidant enzymes such as catalase (CAT), superoxide dismutase (SOD) were depleted in DLA bearing mice and increased significantly near to normal when treated with AuNPI3Cs. From this observation it is clearly evident that AuNPI3Cs induce apoptosis in tumour cells without affecting the normal cells.

6.5 Conclusion

The results showed that AuNPI3Cs possess selective cytotoxicity towards Dalton ascites lymphoma (DLA) cells, which induce apoptosis in a dose-dependent manner. The

apoptogenic effect of AuNPI3Cs may appear via the mitochondrial intrinsic pathway. The antitumor activity noticed in Swiss albino model strongly may be due to antioxidant properties of AuNPI3Cs.